A Journal of the Gesellschaft Deutscher Chemiker

Angewandte International Edition GDCh Chemie

www.angewandte.org

Accepted Article

Title: Photoactivated in situ Generation of Near Infrared Cyanines for Spatiotemporally Controlled Fluorescence Imaging in Living Cells

Authors: Shu Wang

To be cited as: *Angew. Chem. Int. Ed.* 10.1002/anie.202103706

Link to VoR: https://doi.org/10.1002/anie.202103706

WILEY-VCH

10.1002/anie.202103706

COMMUNICATION

WILEY-VCH

Photoactivated *in situ* Generation of Near Infrared Cyanines for Spatiotemporally Controlled Fluorescence Imaging in Living Cells

Gang Song,[a,b,#] Hao Heng,[a,#] Jiaqi Wang,[a] Ronghua Liu,[b] Yiming Huang,[b] Huan Lu,[b] Ke Du,[a] Fude Feng[a] and Shu Wang[b]**

[a] G. Song, H. Heng, K. Du, J. Wang, Prof. Dr. F. Feng
Department of Polymer Science & Engineering, School of Chemistry and Chemical Engineering, Nanjing University, Jiangsu, Nanjing 210023 (P. R. China)
E-mail: fengfd@nju.edu.cn

[b] G. Song, R. Liu, Y. Huang, H. Lu, Prof. Dr. S. Wang
Beijing National Laboratory for Molecular Sciences, Key Laboratory of Organic Solids, Institute of Chemistry, Chinese Academy of Sciences, Beijing, 100190 (P. R. China)
E-mail: wangshu@iccas.ac.cn

[#] G. Song and H. Heng contributed equally.

Supporting information for this article is given via a link at the end of the document.

Abstract: Photoactivated trimerization of 2,3,3-trimethyl-3*H*-indole derivatives created near infrared fluorophore Cy5. The synthetic method is air-tolerant, photosensitizer free, metal free, and condensation agent free. Living cells make Cy5 on a time scale of minutes under white light irradiation at a low power intensity, with the monomer as the only exogenous agent. The new method is promising to find applications in cell studies for *in situ* spatiotemporally controlled fluorescence imaging in living cells.

Fluorescence imaging method is an important tool for detecting and tracking cells or organelles, and has challenging requirements in resolution and specificity.[1] One of promising application in chemical biology is to detect the activity of cells by spatiotemporally controlled fluorescence imaging at the molecular level[2] (e.g., imaging organelles[3-6], tracking the distribution and activation of prodrugs and signaling molecules,[7] monitoring the dynamics of gene regulation,[8] and tuning chemical reactions as well as life processes[9]). Significant progress has been made by imaging adenosine triphosphate (ATP),[10] subtle reduced glutathione (GSH) fluctuations,[11] sulfur dioxide (SO_2),[12] nitric oxide (NO) and formaldehyde release,[13] and NADPH oxidase,[14] etc.

Remotely activatable fluorophores have multiple advantages, particularly in good controllability, spatial selectivity and non-invasiveness.[15] Generally, complex modification of fluorophores with light-sensitive motifs is required. Cyanine dyes are widely accepted fluorophores in cell imaging, thanks to the decent photostability and spectral tunability that is compatible with near infrared (NIR) absorption and emission.[16] One of major problems with the known NIR dyes, not limited to cyanines, lies in the large-sized planar geometry and hydrophobic backbones pre-formed before entry into the cells.

An ideal method to circumvent this problem with NIR dyes should satisfy a few requirements: 1) The NIR dyes can be *in situ* formed from low molecular weight precursors in the intracellular environment; 2) One precursor is better than more, relieving the need for extra agents, and 3) The dye formation is remotely controlled, with selective subcellular localization for detectable NIR emission. At present, it is impossible to apply the conventional synthetic methods for Cy5 formation in living cells because of the harsh conditions (high temperature, strong acid/base, free of water, etc.),[17] long reaction time and the need of unsaturated condensation agent[18].

Herein, we reported an innovative strategy to make Cy5 in one pot under mild conditions (Figure 1a), using 1-(3-aminopropyl)-2,3,3-trimethyl-3*H*-indole (TMI) as a starting material in the presence of a succinimidyl ester (NHS ester) that is used to functionalize the side chain of Cy5. We hypothesized a free-radical-participating pseudo-trimerization mechanism for the reaction. Most importantly, the light-driven formation of Cy5 is favored by the subcellular environment (i.e., lysosomes) at 37℃ as compared to the organic solvent systems, which allows for spatiotemporally controlled imaging of living cells by *in situ* generated Cy5 fluorophores.

In chloroform, the mixture of TMI (in a form of bromine salt, Figures 1a; see Figure S1 for absorption spectrum), Th−NHS (the active ester of thiophene, Figure 1a) and triethylamine was almost colorless under dark. However, after irradiation (10 mW cm^{-2}) by white LED light (Figure S2) at 65℃, the solution turned dark blue (Figure 1b). The reaction was monitored by the UV-vis

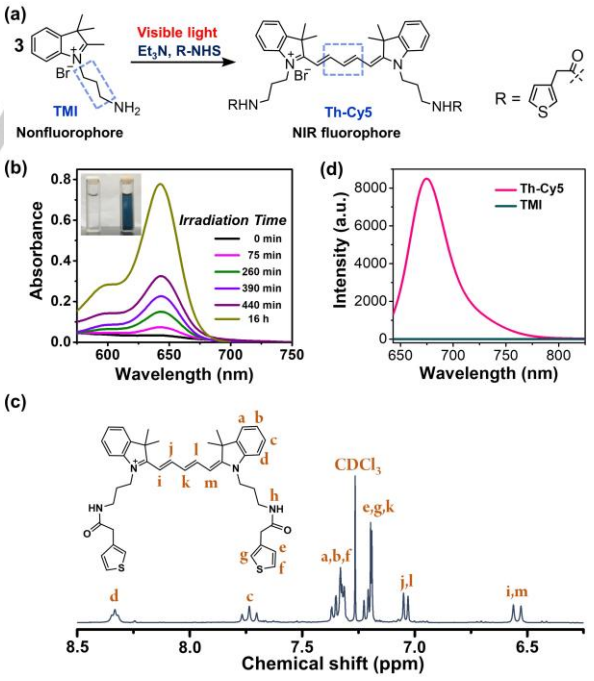

Figure 1. (a) Trimerization of TMI to synthesize Th−Cy5 by a photoactivation strategy. The unsaturated bonds indicated in the square comes from the side chain of TMI. (b) The UV−vis absorption spectra of the reaction solution (diluted by methanol) over time. Inset: photographs of reaction mixture solubilized in methanol before and after photoactivation. (c) ^{1}H NMR spectrum of Th−Cy5 in $CDCl_3$ in the downfield. (d) The fluorescence spectra of TMI (3.6 μM) and Th−Cy5 (3.6 μM) in methanol with excitation at 633 nm.

absorption spectra (Figures 1b, S3). The absorption intensity at 660 nm linearly increased with reaction time (0−10 h) and then plateaued (Figure S4). The blue colored product (Figure S5) was isolated and identified as Th−Cy5 (Figure 1a) through HRMS (Figure S6) and NMR characterizations (Figures 1c, S7&8). In methanol, Th−Cy5 showed strong emission with maximum at 675 nm (Figure 1d), while TMI was non-fluorescent. Due to the low power density of LED light for irradiation and weak absorption of Cy5 dye in the visible region (Figures S1-S2), Th-Cy5 showed excellent photostability against light exposure (Figure S9). The yields were lowered as methanol or ethanol was used as reaction solvent (Table S1). Tertiary amines such as triethylamine, diisopropylethylamine (DIPEA) and triethanolamine (TEOA), supplied in a molar ratio (amine to TMI) of 2:1 (Figure S10), gave rise to similar yields (Table S2). It is noted that this reaction could not be accelerated by regular photosensitizers like camphorquinon, $Ru(bpy)_3Cl_2$, Rhodamine B and Eosin Y (Table S3). The inhibition by 2,2,6,6-tetramethylpiperidine-1-oxyl (TEMPO, a free radical trapping agent)[19] suggested that free radical intermediates likely play a crucial role in the Cy5 formation. The TMI→Th−Cy5 conversion was not affected by air.

To detect free radical intermediates photogenerated from TMI, we performed electron spin resonance (ESR) measurements[20] for the solution of TMI in anhydrous ethanol at room temperature, using 5,5-dimethyl-1-pyrroline-1-oxide (DMPO)[21] as the spin trapping agent. Without light irradiation, even under the heating condition, the solution showed only noise signal in the 3320−3390 G region (Figures 2a, S11-12). In contrast, a six-line signal showed up after 5-min light irradiation, and became more intensified as irradiation time was prolonged to 10 min (Figure 2a) due to accumulation of photogenerated free radical species. According to the pattern of ESR signal, the $\alpha_{\beta\text{-}H}$ and α_N values were calculated as 22.1 G and 14.8 G, respectively, agreeing with the formation of carbon-centered free radicals.[22] We deduced that TMI• radicals were photogenerated and trapped by DMPO to form adduct that was isolatable to be identified by ^{1}H NMR (Figure 2b) and HRMS (m/z 330.2539, Figure 2c). Comparing the ^{1}H NMR data of adduct and TMI (Figure 2b), the $-(CH_2)_3-$ group remained intact. The 2-methyl group possessing active hydrogen could be the adduction site, rather than the $-(CH_2)_3-$ group. However, with the $-NH_2$ replaced by $-CH_3$ at the terminal of side chain, another molecule 1-butyl-2,3,3-trimethyl-3*H*-indole, (termed TMI-CH_3, Figure S13) seemed unreactive to DMPO under light irradiation, showing undetectable ESR signal, likely attributed to the instability of carbon radical formed after removal of the active hydrogen via hydrogen atom transfer (HAT) in the presence of photoexcited TMI-CH_3. Therefore, $-NH_2$ terminated side chain of TMI could help stabilize the radical that is easier to be captured by DMPO (Figure 2d).

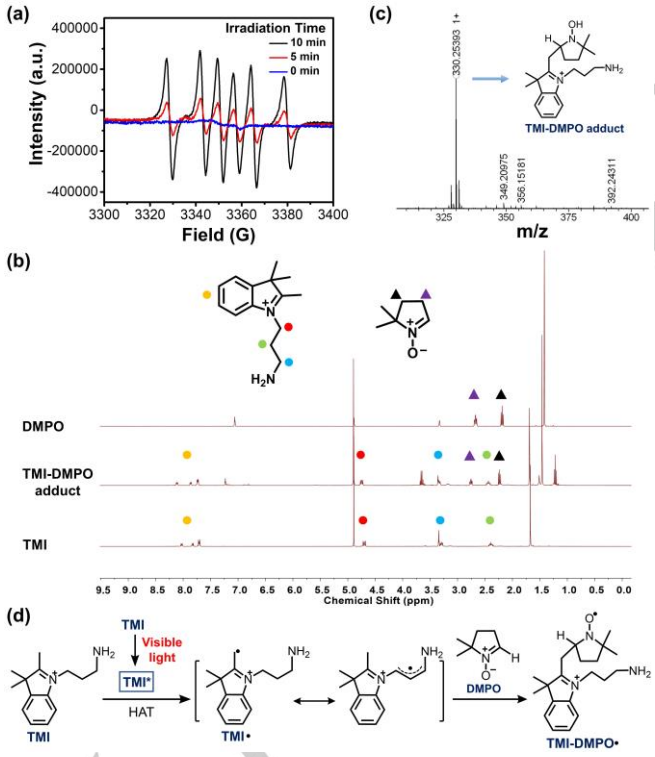

Figure 2. (a) ESR spectra of DMPO spin adducts of photolyzed TMI in anhydrous ethanol for 0−10 min. The *g* factor is 2.01107. (b) ^{1}H NMR spectra of DMPO, TMI and isolated TMI-DMPO adduct (from reaction with ethanol as solvent) in CD_3OD. (c) HRMS analysis of TMI-DMPO adduct. (d) Plausible mechanism for the formation of TMI-DMPO• under light irradiation.

HRMS data of photoproduct from the mixture of TMI and DMPO provided more details of reaction. Particularly, small amounts of Br-TMI-DMPO and TMI-TMI-Br adducts were detected at m/z 432.1620 ($[M+Na]^+$) and 513.2585 ($[M]^+$) (Figure S14), respectively, which suggested more than one HAT steps could take place.

Taken together, we proposed an overall reaction mechanism for Th−TMI→Th−Cy5 (Figure 3), where Th−TMI was generated from the reaction between TMI and NHS ester. The formation of **i1•** is driven by the HAT process (in solvent like chloroform[23]) mediated by the photoexcited TMI (termed TMI*, acting as a photocatalyst). The tautomerized form of **i1•** preserves the active hydrogen at the 2-methyl site and allows for the second round of HAT process with TMI* to generate biradical **i2••**, which rapidly converts into nonradical **i3**. Then **i3** reacts with Th-TMI to form **i4** via Michael addition in the presence of base, thanks to the high activity of methyl group[24] in the TMI moiety. The following steps include $-NH_2R$ removal and a second round of Michael addition and finally form fluorophore Th−Cy5. The whole process was simplified as a trimerization, with the TMI derivative as a monomer.

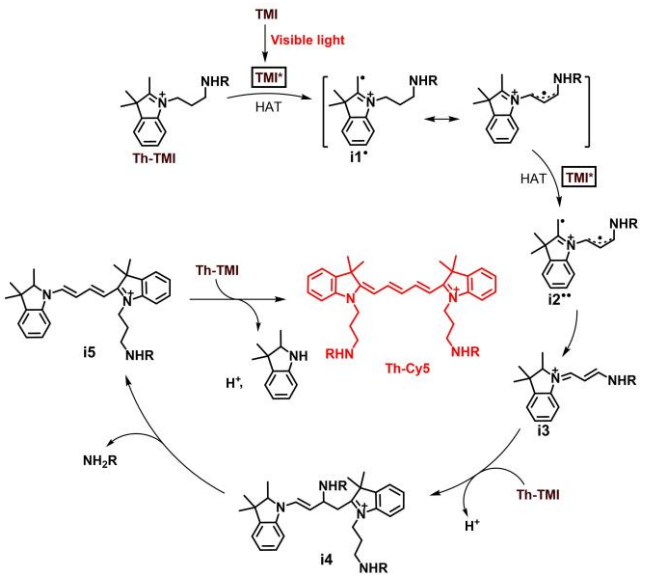

Figure 3. Plausible mechanism for photoactivated Cy5 generation.

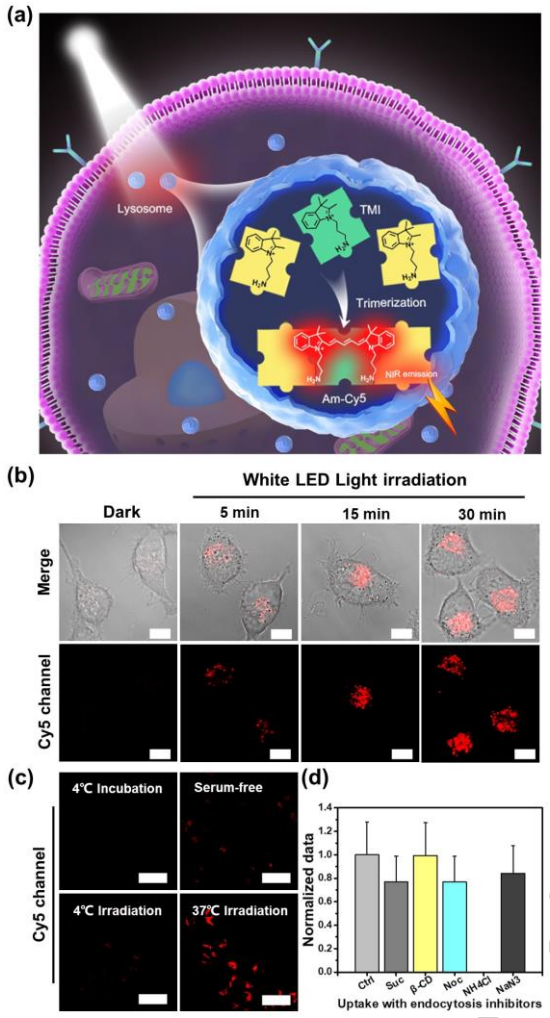

Figure 4. (a) Presentation of in situ generation of Am-Cy5 in the lysosome. (b) CLSM images of TMI-treated HeLa cells with or without white LED light irradiation. Scale bars, 10 μm. (c) CLSM images of TMI-treated HeLa cells under different conditions. Top left: incubation at 4℃ followed by irradiation for 30 min at 37℃; Bottom left: irradiation for 30 min at 4℃; Top right: irradiation for 30 min at 37℃ in serum-free culture medium; Bottom right: irradiation for 30 min at 37 ℃ in serum-supplemented culture medium. Scale bars, 20 μm. (d) Effect of different endocytosis inhibitors. HeLa Cells were incubated with medium containing 450 mM sucrose (Suc), 5 mM β−cyclodextrin (β−CD), 40 μM nocodazole (Noc), 50 mM NH_4Cl, or 0.01% w/v NaN_3 for 2 h before incubation with TMI. Fluorescence intensity in the red channel was measured after 30-min light irradiation. Control (100%): no inhibitors.

Unlike regular phosphate buffer saline that was unfavorable for the reaction (Figure S15), the intracellular environment has some potential advantages: 1) enrichment of reactants in special organelles to reach high local concentrations; 2) availability of enzymes to catalyze complex reactions; 3) intrinsic buffering and redox environments to facilitate oxidation-reduction reactions. Interestingly, endogenous oxidants (e.g., O_2) or reductants (e.g., mM level of GSH) did not disrupt the reaction in the flask (Figure S16), which revealed the Cy5 synthesis reaction could tolerate redox environment. With the above assumption in mind, we investigated the light-driven Cy5 formation in living cells by detecting the NIR fluorescence of Cy5 intracellularly generated (Figure 4a).

Confocal laser scanning microscopy (CLSM) was employed to image living HeLa cells in the red channel with emission collected in the NIR region by excitation at 633 nm. Concerning the nonspecific reactivity to amine species in the cell system, Th−NHS was not applied. To rule out the possibility of extracellular photoactivation, the TMI-treated cells were rinsed three times before light treatment. As a control, non-treated HeLa cells were completely non-emissive. In contrast, after brief white LED light irradiation (50 mW cm^{-2} for 5, 15 and 30 min) on the TMI-treated cells, NIR fluorescence was detected and intensified with increase of irradiation time (Figure 4b) to indicate the formation of emissive Cy5 species in the living cells at 37℃ even at the absence of exogenous tertiary amine. The 3-aminopropyl-substituted Cy5 (termed Am−Cy5, Figure 4a) was detected from cell lysate by mass spectrometry (m/z 469.85) and fluorescence spectrum (Figure S17). TEOA was nontoxic to HeLa cells (Figure S18) and minimally affected the fluorescence intensity using the same procedure (Figure S19). Thereby the need for exogenous tertiary amines was eliminated. Consequently, TMI is the only exogenous substance, with low cytotoxicity with or without LED light irradiation (Figure S20, S21), required for the Cy5 formation in the cells.

To understand the interaction between TMI and cells, we investigated the transport of TMI by imaging cells with CLSM. First, for cells incubated or irradiated by LED light at low temperature (4℃), Cy5 formation was blocked (Figure 4c). Serum components facilitated uptake of TMI, as Cy5 fluorescence was rather weak in serum-free medium as compared to the positive control supplied with serum. According to the isothermal titration calorimetry (ITC) experiment (Figure S22), TMI could bind bovine serum protein (BSA) with a binding constant (k_a) of 2.5 × 10^3 M^{-1} in PBS or 3.4 × 10^4 M^{-1} in water, which means the serum protein could favor cellular uptake of TMI via endocytosis of TMI/serum protein complex. The binding of TMI by serum components was also confirmed by ultrafiltration experiment (Figure S23), which showed serum proteins could bind nearly 52% TMI in the TMI (2 mM)/10% serum mixture. Next, the cells were preincubated with sucrose (inhibitor of clathrin-mediated endocytosis),[25] β−cyclodextrin (inhibitor of caveolae-dependent endocytosis),[26] nocodazole (inhibitor of microtubule polymerization),[27] or NaN_3 (inhibitor of ATPase)[28] before light irradiation. The fluorescence intensity was reduced for the cells treated with sucrose, nocodazole or NaN_3 (Figure 4d), revealing that Cy5 formation is associated with endocytosis. In addition, pre-treatment by 30% sucrose (w/v, sucrose to culture medium)[29] showed negligible impact on the Cy5 fluorescence intensity, reflecting that the diffusion pathway for TMI transport is not responsible for Cy5 formation (Figure S24).

Interestingly, for HeLa cells pre-treated by NH_4Cl that alkalinizes lysosomes and inhibits lysosome activity,[30] no Cy5 signal was detected. The lysosomes extracted from the cells treated with TMI in the presence of serum were fluorescently responsive to visible light at 37℃ in a t_{irr}-dependent manner (Figure S25). These findings suggested the pivotal role of lysosome compartments in photogeneration of Cy5 in living cells. The above results demonstrated substantial improvement of Cy5 generation in the cells as compared to the reaction in the flask, as most of strict conditions were waived. However, consistent to the reaction in the flask (Figure S26), trimerization of TMI-CH_3 could not occur in HeLa cells (Figure S27).

To investigate the spatial distribution of Cy5 product, we carried out CLSM imaging by analyzing the colocalization of

fluorescence signals between the red channel (for Cy5) and green channel (for organelle-specific trackers). The imaging data revealed that the Cy5 product was selectively located in lysosomes (Figures 5a, b and S28&29), rather than other organelles such as Golgi apparatus and mitochondria (Figure S30). It is noteworthy that the signal was stable after 24 h, and remained detectable after 72 h (Figure S31), which showed good photostability of *in situ* generated Cy5 promising for long term cell imaging.

To quantify the level of Cy5 synthesized in cells, or more specifically in the lysosomes, we compared photogenerated Am-Cy5 with commercial BSA-Cy5 in the fluorescence intensity intracellularly using the same procedures. BSA-Cy5 is internalized via endocytosis in the similar pattern with serum protein complexed TMI. In the same microenvironment (i.e., lysosomes) BSA-Cy5 and Am-Cy5 are assumed to have comparable fluorescence quantum yields, which makes it possible to estimate the amount of Am-Cy5 according to the BSA-Cy5 based standard curve from BSA-Cy5 treated cells after removal of extracellular medium and various-fold dilutions (Figures 5c-d). On the basis that tumor cells could uptake 20% BSA-Cy5 after 30-min incubation,[31] the Am-Cy5 generated from TMI in cells was calculated as approximately 0.16 μM. Therefore, roughly 0.5% of total TMI was converted into Am-Cy5.

In summary, we have developed a novel method to synthesize Cy5 fluorophores through photoactivation of TMI by white LED light, and proposed a free radical-participating trimerization mechanism to interpret the formation of conjugated backbone from the *N*-alkyl side chain. We reported that living cells taking up TMI can form Cy5 selectively in the lysosome compartments without the need for any exogenous agent except visible light, which allows for spatiotemporal imaging of living cells by virtue of the NIR fluorescence from the *in situ* photogenerated Cy5. Although there are limitations in understanding the exact mechanism how living environments lead to Cy5 generation under mild conditions as compared to the reaction in the flask, this method provides a new chemical toolbox for cell studies.

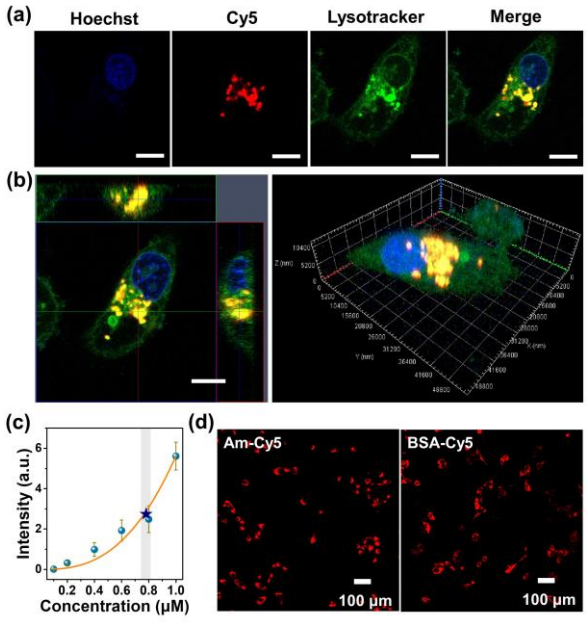

Figure 5. (a) CLSM images of TMI-treated HeLa cells after white LED light irradiation for 30 min. Scale bars, 10 μm. Blue channel: λ_{ex} = 405 nm, λ_{em} = 415−450 nm; Green channel: λ_{ex} = 488 nm, λ_{em} = 500−600 nm; Red channel: λ_{ex} = 633 nm, λ_{em} = 650−750 nm. (b) 3D (Z-stacks) CLSM images of HeLa cells. Scale bar, 10 μm. (c) The plot of fluorescence intensity of BSA-Cy5 treated cells as a function of BSA-Cy5 concentration (based on Cy5 moiety). The pentagram mark represented the fluorescence intensity of TMI-treated cells. (d) CLSM images of TMI-treated (0.1 mM, left) and BSA-Cy5-treated (0.8 μM, right) HeLa cells. Scale bar, 100 μm.

Acknowledgements

We are grateful to Yutan Shen, Prof. Yilin Wang (Institute of Chemistry, Chinese Academy of Sciences) for the help with ITC measurements. We thank National Key R&D Program of China (2017YFA0701301, 2018YFE0200700), National Natural Science Foundation of China (22021002, 22077065), Program for Changjiang Scholars and Innovative Research Team in University for financial support.

Keywords: Photoactivation • cyanine dyes • near infrared fluorescence imaging • in situ synthesis • lysosome

[1] a) M. Gao, F. Yu, C. Lv, J. Choo, L. Chen, *Chem. Soc. Rev*. **2017**, *46*, 2237−2271; b) Q. Shao, B. Xing, *Chem. Soc. Rev.* **2010**, *39*, 2835−2846.
[2] H. Chu, J. Zhao, Y. Mi, Y. Zhao, L. Li, *Angew. Chem. Int. Ed.* **2019**, *58*, 14877−14881.
[3] P. An, Z. Yu, Q. Lin, *Chem. Commun*. **2013**, *49*, 9920−9922.
[4] a) J. Lee, K. Kim, H. Jin, Y. Baek, Y. Choi, S. Jung, S. Lee, J. Bae, J. Jung, *ACS Appl. Mater. Interfaces* **2018**, *10*, 3380−3391; b) H. He, J. Wang, H. Wang, N. Zhou, D. Yang, D. R. Green, B. Xu, *J. Am. Chem. Soc*. **2018**, *140*, 1215−1218; c) G. Feng, J. Liu, C. J. Zhang, B. Liu, *ACS Appl. Mater. Interfaces* **2018**, *10*, 11546−11553.
[5] a) R. S. Li, P. F. Gao, H. Z. Zhang, L. L. Zheng, C. M. Li, J. Wang, Y. F. Li, F. Liu, N. Li, C. Z. Huang, *Chem. Sci.*, **2017**, *8*, 6829−6835; b) R. S. Kathayat, Y. Cao, P. D. Elvira, P. A. Sandoz, M. E. Zaballa, M. Z. Springer, L. E. Drake, K. F. Macleod, F. G. van der Goot, B. C. Dickinson, *Nat. Commun*. **2018**, *9*, 334−348; c) P. Li, X. Guo, X. Bai, X. Wang, Q. Ding, W. Zhang, W. Zhang, B. Tang, *Anal. Chem*. **2019**, *91*, 3382−3388.
[6] a) Z. Feng, H. Wang, S. Wang, Q. Zhang, X. Zhang, A. A. Rodal, B. Xu, *J. Am. Chem. Soc.* **2018**, *140*, 9566−9573; b) B. Dong, Y. Lu, N. Zhang, W. Song, W. Lin, *Anal. Chem*. **2019**, *91*, 5513−5516.
[7] M. Ye, X. Wang, J. Tang, Z. Guo, Y. Shen, H. Tian, W. H. Zhu, *Chem. Sci.* **2016**, *7*, 4958−4965.
[8] W. Zhou, W. Brown, A. Bardhan, M. Delaney, A. S. Ilk, R. R. Rauen, S. I. Kahn, M. Tsang, *Angew. Chem. Int. Ed*. **2020**, *59*, 8998−9003.
[9] M. Bezagu, C. Errico, V. Chaulot-Talmon, F. Monti, M. Tanter, P. Tabeling, J. Cossy, S. Arseniyadis, O. Couture, *J. Am. Chem. Soc*. **2014**, *136*, 7205−7208.
[10] S. Hong, X. Zhang, R. J. Lake, G. T. Pawel, Z. Guo, R. Pei, Y. Lu, *Chem. Sci*. **2020**, *11*, 713−720.
[11] H. Zong, J. Peng, X. R. Li, M. Liu, Y. Hu, J. Li, Y. Zang, X. Li, T. D. James, *Chem. Commun*. **2020**, *56*, 515−518.
[12] W. Zhang, F. Huo, Y. Yue, Y. Zhang, J. Chao, F. Cheng, C. Yin, *J. Am. Chem. Soc*. **2020**, *142*, 3262−3268.
[13] a) X. Xie, J. Fan, M. Liang, Y. Li, X. Jiao, X. Wang, B. Tang, *Chem. Commun*. **2017**, *53*, 11941−11944; b) L. P. Smaga, N. W. Pino, G. E. Ibarra, V. Krishnamurthy, J. Chan, *J. Am. Chem. Soc*. **2020**, *142*, 680−684.
[14] W. Chang, Y. Yang, H. Lu, I. Li, I. Liau, *J. Am. Chem. Soc*. **2010**, *132*, 1744−1745.
[15] a) J. Zhao, H. Chu, Y. Zhao, Y. Lu, L. Li, *J. Am. Chem. Soc*. **2019**, *141*, 7056−7062; b) A. K. Rudd, J. M. Valls Cuevas, N. K. Devaraj, *J. Am. Chem. Soc*. **2015**, *137*, 4884−4887.
[16] a) Z. Lei, C. Sun, P. Pei, S. Wang, D. Li, X. Zhang, F. Zhang, *Angew. Chem. Int. Ed*. **2019**, *58*, 8166−8171; b) M. Matsui, T. Yamamoto, Y. Kubota, K. Funabiki, *New J. Chem*. **2016**, *40*, 10187−10196; c) K. Mitra, C. E. Lyons, M. C. T. Hartman, *Angew. Chem. Int. Ed*. **2018**, *57*, 10263−10267; d) C. Sun, B. Li, M. Zhao, S. Wang, Z. Lei, L. Lu, H. Zhang, L. Feng, C. Dou, D. Yin, H. Xu, Y. Cheng, F. Zhang, *J. Am. Chem. Soc*. **2019**, *141*, 49, 19221−19225; e) S. Wang, Y. Fan, D. Li, C. Sun, Z. Lei, L. Lu, T. Wang, F. Zhang, *Nat. Commun.* **2019**, *10*, 1058.
[17] Brooker, L. G. S. *J. Am. Chem. Soc*. **1965**, *87*, 937−938.
[18] A. Toutchkine, P. Nalbant, K. M. Hahn, *Bioconjugate Chem*. **2002**, *13*, 387−391.
[19] T. Li, K. Liang, Y. Zhang, D. Hu, Z. Ma, C. Xia, *Org. Lett.* **2020**, *22*, 2386−2390.

[20] K. Kruczala, J. G. Bokria, S. Schlick, *Macromolecules*. **2003**, *36*, 1909−1919.
[21] J. Clément, N. Ferré, D. Siri, H. Karoui, A. Rockenbauer, P. J. Tordo, *J. Org. Chem*. **2005**, *70*, 1198−1203.
[22] a) X. Q. Wang, F. Gao, X. Z. Zhang, *Angew. Chem. Int. Ed*. **2017**, *56*, 9029−9033; b) W. Q. Liu, T. Lei, Z. Q. Song, X. L. Yang, C. J. Wu, X. Jiang, B. Chen, C. H. Tung, L. Z. Wu, *Org. Lett*. **2017**, *19*, 3251−3254; c) M. B. Kadiiska, K. S. D. Costa, R. P. Mason, J. M. Mathews, *Chem. Res. Toxicol*. **2000**, *13*, 1082−1086.
[23] K. Makhal, S. Maurya, D. Goswami, *Physica Scripta* **2019**, *94*, 9.
[24] L. Zhang, J. C. Er, X. Li, J. J. Heng, A. Samanta, Y. T. Chang, C. L. Lee, *Chem. Commun*. **2015**, *51*, 7386−7389.
[25] Li. Li, S. Qiao, W. Liu, Y. Ma, D. Wan, J. Pan, H. Wang. *Nat. Commun*. **2017**, *8*, 1276.
[26] G. Gasparini, E. K. Bang, G. Molinard, D. V. Tulumello, S. Ward, S. O. Kelley, A. Roux, N. Sakai, S. Matile, *J. Am. Chem. Soc*. **2014**, *136*, 6069−6074.
[27] Y. Tsubono, Y. Kawamoto, T. Hidaka, G. N. Pandian, K. Hashiya, T. Bando, H. Sugiyama, *J. Am. Chem. Soc.* **2020**, *142*, 17356−17363.
[28] D. Mandal, A. Nasrolahi Shirazi, K. Parang, *Angew. Chem. Int. Ed*. **2011**, *50*, 9633−9637.
[29] C. Li, M. Yu, Y. Sun, Y. Wu, C. Huang, F. Li, *J. Am. Chem. Soc*. **2011**, *133*, 11231−11239.
[30] K. Sakamoto, M. Akishiba, T. Iwata, K. Murata, S. Mizuno, K. Kawano, M. Imanishi, F. Sugiyama, S. Futaki, *Angew. Chem. Int. Ed*. **2020**, *59*, 19990−19998.
[31] H. Zhang, Z. Sun, K. Wang, N. Li, H. Chen, X. Tan, L. Li, Z. He, J. Sun, *Bioconjugate Chem*. **2018**, *29*, 1852−1858.

10.1002/anie.202103706

Entry for the Table of Contents

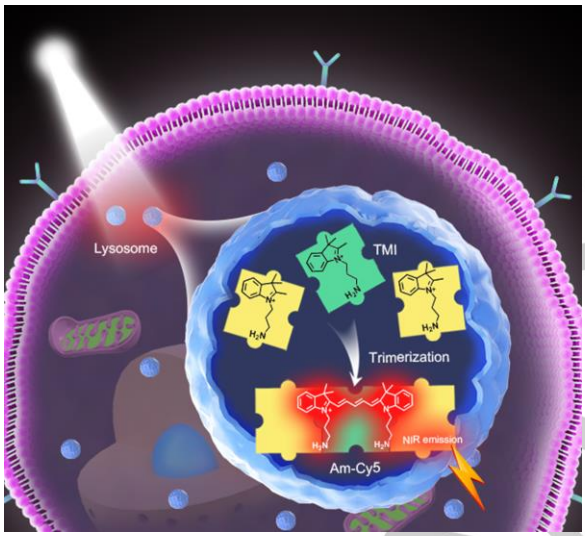

A visible light-driven photochemical method was designed for one-pot synthesis of Cy5 fluorophore via carbon radical-participating trimerization under mild conditions, by virtue of self-photocatalytic activity of 2,3,3-trimethyl-3*H*-indole derivatives. The in situ photochemical reaction could occur selectively in the lysosomes of living cells in an irradiation time-dependent manner with only one exogenous substrate, potentially applicable for spatiotemporally controlled fluorescence imaging in living cells.